3944–3949 *Nucleic Acids Research, 1997, Vol. 25, No. 19*

Localization of the major ethidium bromide binding site on tRNA

Wen-Chy Chu*, Jack C.-H. Liu and Jack Horowitz

Department of Biochemistry and Biophysics, Iowa State University, Ames, Iowa 50011, USA

Received May 15, 1997; Accepted August 11, 1997

ABSTRACT

Binding of ethidium bromide to *Escherichia coli* tRNA^{Val} and an RNA minihelix based on the acceptor stem and T-arm of tRNA^{Val} was investigated by ^{19}F and ^{1}H NMR spectroscopy of RNAs labeled with fluorine by incorporation of 5-fluorouracil. Ethidium bromide selectively intercalates into the acceptor stem of the tRNA^{Val}. More than one ethidium bromide binding site is found in the acceptor stem, the strongest between base pairs A6:U67 and U7:A66. ^{19}F and ^{1}H spectra of the 5-fluorouracil-substituted minihelix RNA indicate that the molecule exists in solution as a 12 base-paired stem and a single-stranded loop. Ethidium bromide no longer intercalates between base pairs corresponding to the tRNA^{Val} acceptor stem in this molecule. Instead, it intercalates between base pairs at the bottom of the long stem–loop structure. These observations suggest that ethidium bromide has a preferred intercalation site close to the base of an RNA helical stem.

INTRODUCTION

Binding of ethidium bromide (EB) to polynucleotides has been extensively studied because the drug acts as a potential mutagen and antibiotic (1), exhibits effective antiviral activity (2), inhibits protein and nucleic acid synthesis, and affects the biological activity of DNA and RNA (3–6). EB interacts strongly with double-stranded DNA and RNA and is widely used as a probe of nucleic acid structure (7–10). The predominant mode of EB binding to double-stranded polynucleotides is by intercalation between adjacent base pairs (11). Because tRNAs exhibit a diversity of well characterized secondary and tertiary structural features, they have often been used as models for studying RNA–drug interactions (12–19).

Results of proton nuclear magnetic resonance (NMR) (12,13), fluorescence lifetime (14) and singlet–singlet energy transfer (15,16) measurements of the binding of EB to tRNA suggest that the dye intercalates between base pairs at the base of the acceptor stem. However, an X-ray diffraction study of the structure of the yeast tRNA^{Phe}–EB complex (17), ^{31}P NMR studies of EB binding to tRNA^{Phe} (18), and nuclease probes of the EB-tRNA^{Phe} complex (19) favor a non-intercalative mode of EB binding in a cavity at the mouth of the P10 loop within the tertiary structure of the tRNA (17). To help resolve these differences and to better understand the mechanism of EB binding, the interaction of EB with *Escherichia coli* tRNA^{Val} and an RNA minihelix corresponding to the acceptor stem and T-arm of tRNA^{Val} was examined by ^{1}H and ^{19}F NMR.

^{19}F NMR is a powerful probe of the solution structure of tRNA labeled by incorporation of 5-fluorouracil (FUra) (20–27). The 14 FUra residues in FUra-substituted *E.coli* tRNA^{Val} [(FUra)tRNA^{Val}] are distributed throughout all stems and loops of the molecule (Fig. 1A). Its ^{19}F NMR spectrum shows a resolved resonance for each incorporated fluorine and these have now been completely assigned (25,28,29). The high sensitivity of the ^{19}F nucleus and the well-resolved ^{19}F NMR spectrum of (FUra)tRNA^{Val} permit a clear, unambiguous determination of EB binding sites in the tRNA molecule. The results reported here reveal a structural preference for the binding of EB into sites close to the base of RNA helical stems.

MATERIALS AND METHODS

Preparation of the DNA template for *in vitro* transcription of *E.coli* tRNA^{Val} by T7 RNA polymerase was as described previously (30). The gene for the minihelix, consisting of the acceptor stem and T-arm sequence of tRNA^{Val}, was constructed by deletion mutagenesis (31) using a 30mer mutagenic primer (synthesized by the Nucleic Acid Facility at Iowa State University) corresponding to the 15 base sequence flanking the region of the tRNA gene to be deleted. RNA was transcribed *in vitro* as described (25), except the concentration of nucleotide triphosphates was 3 mM for transcription of the minihelix. Numbering of the minihelix follows that of the corresponding sequence in intact tRNA^{Val} to facilitate comparison (Fig. 1). 5-Fluorouridine triphosphate (FUTP) replaced UTP for transcription of FUra-substituted RNAs. Transcripts were first chromatographed on a TSK-DEAE high pressure liquid chromatography (HPLC) column and were then further purified on a C4-reversed phase HPLC column (25). Transfer RNA samples accepted valine at a level of at least 1000 pmol/A_{260}. Bisulfite modification of the RNA minihelix was carried out by established procedures (21).

HPLC gel filtration chromatography was used to establish the size of minihelices in solution; size standards used were: adenosine (1mer), GUAA (4mer), oligoriboadenylic acid decamer (10mer), microhelix (22mer) and wild-type tRNA^{Val} (76mer). All samples were dissolved in standard NMR buffer and chromatographed at

*To whom correspondence should be addressed. Tel: +1 515 294 1813; Fax: +1 515 294 1597; Email: wchu@iastate.edu

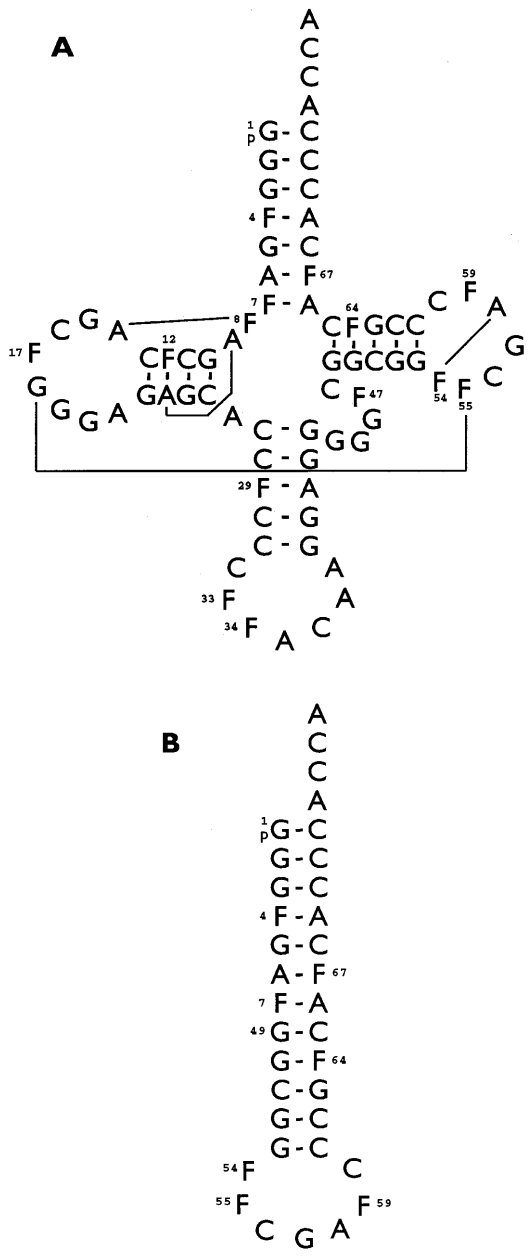

Figure 1. Structures of *in vitro* transcribed *E.coli* tRNA^{Val} (**A**) and minihelix tRNA^{Val} represented by a hairpin–loop structure (**B**) with uracil replaced by FUra (F). Tertiary base pairs involving FUra are connected by solid lines. The nucleotide positions in the minihelix are labeled to correspond with full length tRNA^{Val}.

22°C on an Altex Spherogel-TSK column. Elution volume for each sample was recorded, and the relation of elution volumes and log values of nucleotide number was determined.

For NMR spectroscopy, tRNA samples were dissolved in a minimum volume of standard buffer (50 mM sodium cacodylate, pH 6.0, 15 mM $MgCl_2$, 100 mM NaCl and 1 mM EDTA) and were then dialyzed against two changes of the same buffer. After dialysis, the sample volume was adjusted to 0.405 ml, and 10% (v/v) D_2O was added to serve as an internal lock signal. RNA was renatured prior to recording NMR spectra by heating the samples to 55°C for 20 min and allowing them to cool slowly to room temperature. EB (Sigma) was added as small aliquots of a concentrated stock solution (20 mM) prepared in standard buffer. Transfer RNA concentration was determined by using $A^{0.1\%}_{260}$ = 24. The molecular mass of full length tRNA^{Val} = 26 kDa and that of the minihelix = 12 kDa.

All NMR spectra were obtained on a Varian Unity 500 FT NMR spectrometer. ^{19}F NMR spectra were collected at 470 MHz by using 16 K data points, with no relaxation delay and a pulse angle optimizing the Ernst condition (32). An exponential line broadening of 15 Hz was applied before the spectrum was transformed. ^{19}F chemical shifts are reported downfield from free FUra. ^{1}H NMR spectra were collected as described by Kintanar *et al.* (33). A 1–1 spin-echo selective excitation pulse sequence (34) was applied to suppress the water signal. Chemical shifts are related to the water signal, assumed to resonate at 4.80 p.p.m. at 22°C. All spectra were collected at 22°C except as otherwise indicated.

One-dimensional difference NOEs (nuclear Overhauser effects), for assignment of proton resonances in the RNA minihelix, were performed at 10°C with a 0.4 s presaturation pulse followed by a jump–return pulse sequence (35). The presaturation pulse was of sufficient power to saturate 90% of the irradiated peak.

RESULTS

^{19}F NMR spectra of the EB–(FUra)tRNA^{Val} complex

Binding of EB to tRNA^{Val} was monitored by following changes in the ^{19}F NMR spectrum of *in vitro* transcribed (FUra)tRNA^{Val} with increasing EB concentration. The results (Table 1 and Fig. 2) show that resonances arising from FU7, FU67 and FU4 are strongly affected by the addition of EB; FU7 is the most sensitive to EB binding. As the EB concentration is increased, an increasing fraction of peak FU7 shifts upfield from 3.87 to 3.13 p.p.m., to a position between the resonances of FU54 and FU12/29 (Fig. 2). These resonances merge into a single broad peak at higher EB concentrations (Fig. 2). Upfield shifts of increasing fractions of peaks FU67 and FU4 also become evident as the EB/tRNA ratio increases (Fig. 2). FU67 shifts from 2.51 to 1.97 p.p.m. to overlap with FU8, and FU4 shifts from 1.74 to 1.47 p.p.m. Observation of two discrete peaks for all three resonances indicates that each fluorine is in slow exchange on the chemical shift time scale between two magnetically distinct environments.

In addition to the chemical shift changes just described, splitting of a peak in the central region of the spectrum is observed at EB/tRNA ratios >2 (Fig. 2E). To identify the resonance involved, the ^{19}F NMR spectrum of (FUra)tRNA^{Val} was recorded at 47°C where the peaks in this part of the spectrum are better resolved. The results (Fig. 3) show that the intensity of FU47 is diminished as a result of EB binding. An additional effect is a gradual broadening of FU59 and possibly FU55 with increasing EB/tRNA ratios (Figs 2C–E and 3B). The resonance corresponding to FU8, located in the P-10 loop, is not affected by EB binding to tRNA^{Val}.

The results described were obtained with *in vitro* transcripts of tRNA^{Val}, which are devoid of nucleotide modifications. Similar effects were observed with partially modified (FUra)tRNA^{Val} isolated from FUra-treated *E.coli* cells (data not shown).

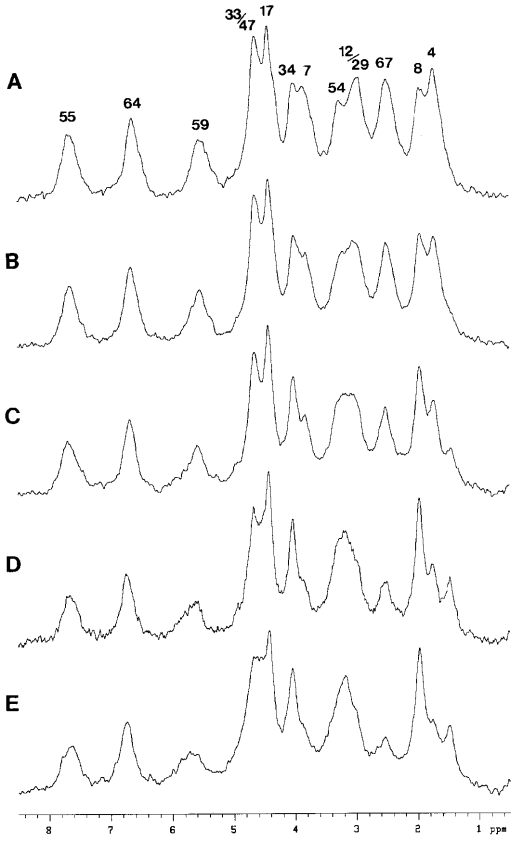

Figure 2. Effect of EB binding on the ^{19}F NMR spectrum of (FUra)tRNA^{Val} (0.17 mM). Spectra were recorded at 22°C in the absence of EB (**A**) and after addition of EB to a molar ratio to tRNA of (**B**) 0.5; (**C**) 1; (**D**) 2; (**E**) 3.

Table 1. ^{19}F chemical shifts of free and EB bound (FUra)tRNA^{Val}

Fluorouracil residue	Chemical shifts (δ) p.p.m. at 22°C			p.p.m. at 47°C		
	free[a]	bound[b]	Δp.p.m.[c]	free[a]	bound[b]	Δp.p.m.[c]
FU55	7.68	7.62	0.06	7.74	7.71	0.03
FU64	6.64	6.73	–0.09	6.78	6.80	–0.02
FU59	5.56	5.60	–0.04	5.83	5.86	–0.03
FU33	4.64	4.67	–0.03	4.89	4.91	–0.02
FU47	4.64	4.55	0.09	4.66	4.62	0.04
FU17	4.44	4.42	0.02	4.50	4.51	–0.01
FU34	4.02	4.04	–0.02	4.33	4.34	–0.01
FU7	3.87	3.13[d]	**0.74**	3.93	3.31	**0.62**
FU54	3.27	n.d.	–	3.46	3.51	–0.05
FU12	2.98	n.d.	–	3.29	3.26	0.03
FU29	2.98	n.d.	–	2.68	2.70	–0.02
FU67	2.51	1.97	**0.54**	2.68	1.94	**0.74**
FU8	1.95	1.97	–0.02	2.26	2.27	–0.01
FU4	1.74	1.47	**0.27**	1.92	1.65	**0.27**

[a]Chemical shifts of (FUra)tRNA^{Val} in the absence of added EB.
[b]Chemical shifts of (FUra)tRNA^{Val} in the presence of 3-fold molar excess of EB.
[c]Δp.p.m. = δ (free tRNA) – δ (EB bound tRNA).
[d]Chemical shift determined at EB/tRNA ratio of 0.5.
n.d., not detected due to overlapping peaks.

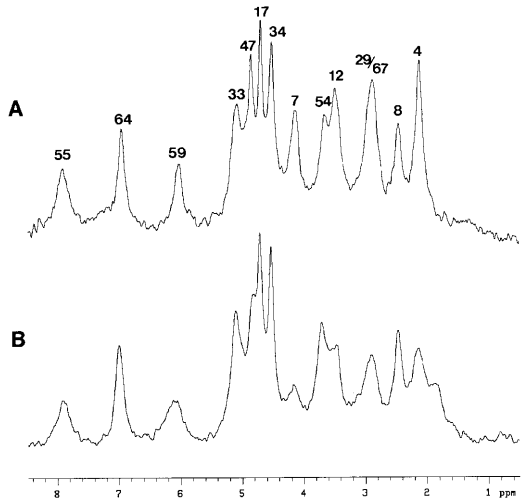

Figure 3. ^{19}F NMR spectra of (FUra)tRNA^{Val} (0.17 mM), recorded at 47°C in the absence of EB (**A**) and in the presence of the dye at a molar ratio to tRNA of 3 (**B**).

^{1}H NMR spectra of the EB–tRNA^{Val} complex

Binding of EB to tRNA^{Val} (not substituted with FUra) was also monitored by ^{1}H NMR (Fig. 4). The results are not as clear-cut as those obtained by ^{19}F NMR, partly because there are 26–28 resonances in the imino proton region of the ^{1}H NMR spectrum of tRNA^{Val}, and it is difficult to follow chemical shifts of the overlapping peaks. Resonances in the proton NMR spectrum of *in vitro* transcribed tRNA^{Val} were recently assigned (36); only those involved in the acceptor stem of tRNA^{Val} are indicated in Figure 4. With increasing EB concentration the intensity of resonances corresponding to the imino protons of the U4:A69, G5:C68, A6:U67 and U7:A66 base pairs decreases (Fig. 4). We have not been able to locate new signals resulting from the shift of these resonances; however, the intensity of the signal at 13.8 p.p.m. increases as EB is added (indicated by an arrow in Fig. 4D). Kearns and co-workers (13) suggested that intercalation of EB causes the imino proton resonances of the affected base pairs to shift upfield, and it is possible that the resonance at 13.8 p.p.m. corresponds to the EB-bound conformer of A6:U67. Imino proton signals from the G1:C72, G2:C71 and G3:C70 base pairs are not affected by EB binding. These results indicate that EB binds to the acceptor stem of normal tRNA^{Val} by intercalating between base pairs 4 and 7.

^{1}H NMR spectra of an EB–minihelix complex

To further delineate the RNA binding site preferences of EB, dye binding to a minihelix having the sequence of the acceptor stem and T-arm of tRNA^{Val} was investigated. Gel filtration chromatography (Altex Spherogel-TSK), established that the minihelix exists as a monomer in solution in standard buffer at the concentrations (0.3 mM) used for NMR experiments (results not shown). The downfield ^{1}H NMR spectrum of the FUra-substituted minihelix, recorded at 22°C, is shown in Figure 5A. Intensity corresponding to 13 imino protons resonances is observed, with 11 well-resolved peaks in the region from 11 to 15 p.p.m. The peaks at 12.53 and 12.00 p.p.m. both have the

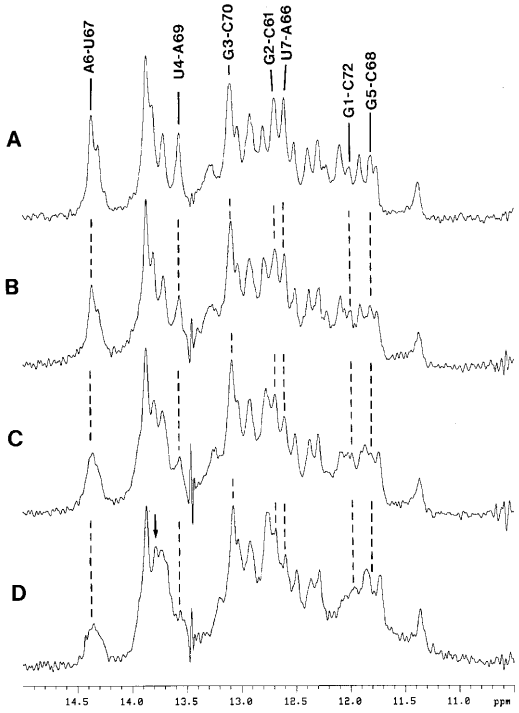

Figure 4. ^{1}H NMR spectrum of normal tRNA^{Val} (0.15 mM) in the absence of EB (**A**); and in the presence of EB at a molar ratio to tRNA of (**B**) 0.5; (**C**) 1; (**D**) 2. Imimo proton resonances of base pairs in the acceptor stem of tRNA^{Val} are labeled.

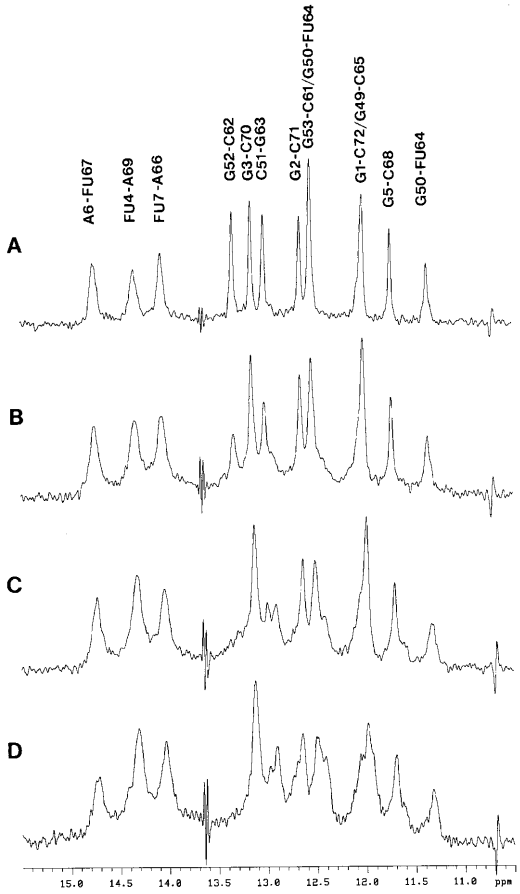

Figure 5. Effect of EB binding on the ^{1}H NMR spectrum of the (FUra)-minihelix. (FUra)minihelix (0.3 mM) in the absence (**A**), and in the presence of EB at a molar ratio to minihelix of: (**B**) 0.5; (**C**) 1; and (**D**) 2.

intensity of two protons, with the latter being resolved into two separate peaks at 37°C. These results indicate that the minihelix has a hairpin loop structure with a stem of 12 contiguous base pairs.

Established procedures (36) were used to assign the imino proton spectrum of the minihelix. The three farthest downfield resonances, between 14 and 15 p.p.m., are in the chemical shift range characteristic of A:U base pairs. Moreover, they each show a fairly strong NOE to a narrow proton peak in the upfield range of aromatic resonances (not shown), which is diagnostic of Watson–Crick A:U base pairs. This permits assignment of the three downfield peaks to the three FU:A base pairs in the minihelix. Two resonances, located at 12.53 and 11.34 p.p.m., exhibit strong reciprocal NOEs (not shown), indicative of a G:FU base pair that contains two imino protons in close proximity. These resonances were, therefore, assigned to the G50:FU64 base pair. Other imino proton resonances were identified by following one-dimensional NOE connectivities from these spectroscopic markers; the results are shown in Figure 5A. The imino proton resonance corresponding to the FU54:A58 reverse Hoogsteen tertiary base pair found in intact tRNA is not observed in the spectrum of the minihelix.

Changes induced in the ^{1}H NMR spectrum of the minihelix upon binding of EB are depicted in Figure 5. As EB is added, an increasing fraction of the resonances corresponding to G52:C62, C51:G63 and one component of the double peak G53-C61/G50-FU64 shift upfield 0.1–0.2 p.p.m. Peak G52:C62 shifts from 13.32 to 13.13 p.p.m., overlapping G3-C70; peak C51-G63 shifts from 13.00 to 12.91 p.p.m., and G53-C61/G50-FU64 shifts from 12.53 to 12.44 p.p.m. All resonances strongly affected by EB binding are assigned to base pairs at the bottom of the helical stem of the minihelix.

^{19}F NMR spectra of an EB–(FUra)minihelix complex

The ^{19}F NMR spectrum of the FUra-substituted minihelix shows six resolved resonances, with the signal at 4.0 p.p.m. (peaks C/D) having the intensity of two fluorines (Fig. 6). These peaks correspond to the seven fluorouracil residues in the minihelix: one in a wobble FU:G base pair, three as FU:A Watson–Crick base pairs, and three unpaired FUra residues in the loop (Fig. 1B). Comparison of the ^{19}F NMR spectrum of the (FUra)minihelix with that of full-length (FUra)tRNA^{Val} (Fig. 6), shows that peaks A, F and G have chemical shifts close to those of FU64, FU67 and FU4 in full-length tRNA^{Val}, permitting assignment of A, F and G to FU64, FU67 and FU4, respectively.

FUras in the loop of the minihelix can be assigned by determining ^{19}F NMR spectral changes resulting from reaction with sodium bisulfite. Bisulfite is known to react preferentially with FUra residues located in single-stranded regions of RNA (21,37) causing the ^{19}F signal to shift 35–40 p.p.m. upfield (21,37). As shown in Figure 6B and C, reaction of the minihelix with bisulfite shifts resonances B, C and D, from the central region of the ^{19}F NMR spectrum upfield to –36 to –38 p.p.m.; the three upfield peaks, E, F and G, remain unaffected by reaction

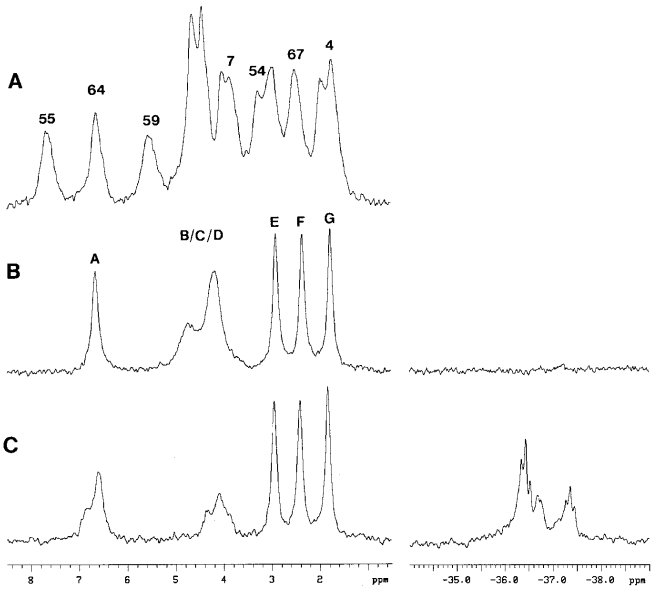

Figure 6. ^{19}F NMR spectrum of: (**A**) full length (FUra)tRNA^{Val}; (**B**) (FUra) minihelix; and (**C**) bisulfite-modified (FUra)minihelix. Only those fluorouracil residues present in the minihelix are labeled in (A).

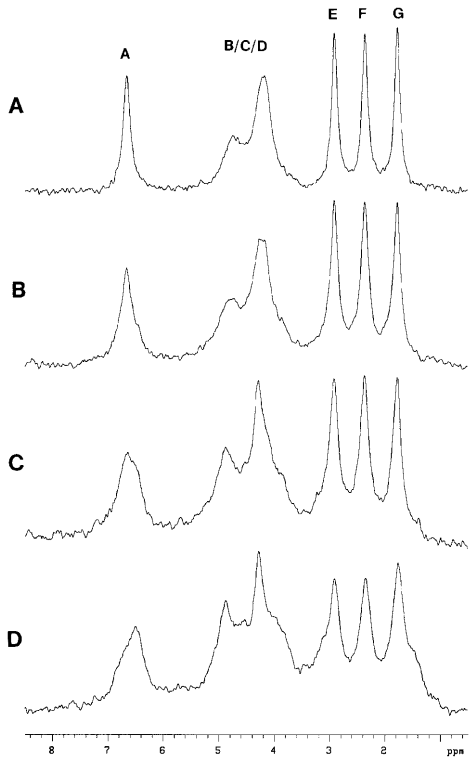

Figure 7. Effect of EB binding on the ^{19}F NMR spectrum of (FUra)-minihelix. (FUra)minihelix (0.3 mM) in the absence (**A**) and in the presence of EB at a molar ratio to minihelix of: (**B**) 0.5; (**C**) 1; and (**D**) 2.

with bisulfite. Peaks B, C and D can therefore be assigned to FU54, FU55 and FU59 in the loop of the minihelix. These resonances are broader than others in the spectrum of the (FUra)minihelix, suggesting that the loop structure in this molecule is in a fast exchanging dynamic state. In full length tRNA^{Val}, signals from the FUra residues at positions 54, 55 and 59 are shifted away from the central region of the ^{19}F spectrum (Figs 2 and 3; refs 28,29). This is presumably because in intact tRNA these fluorouracils are either involved in the tertiary interactions between the D- and T-loops or protected from solvent by these interactions (21,28).

The remaining resonance, peak E, corresponds to FU7. In the ^{19}F NMR spectrum of intact tRNA^{Val}, the peak from FU7 in the FU7:A66 base pair is shifted considerably downfield from the chemical shift position of signals from other FUra residues involved in Watson–Crick base pairing, and appears near the central region of the spectrum. This is probably because the FU7:A66 base pair is only partially stacked on the adjacent G49:C65 base pair at the acceptor stem/T-stem juncture of the L-shaped tRNA molecule (38). It is reasonable to expect that when the FU7:A66 base pair occurs in a regular helix, as it does in the minihelix structure, that the corresponding ^{19}F resonance shifts upfield into the region expected for a FU:A Watson–Crick base pair, thus accounting for the upfield position of peak E in the ^{19}F NMR spectrum of the minihelix relative to that of FU7 in the spectrum of intact tRNA^{Val}.

Assignment of the ^{19}F NMR spectrum of the minihelix is consistent with our previous results correlating ^{19}F chemical shifts with the secondary and tertiary structural environment of fluorouracils incorporated into tRNA (29). From assignment of the spectrum of intact (FUra)tRNA^{Val} we concluded that fluorouracils located in loops of the tRNA resonate in the central region of the spectrum; signals from FUra involved in G:FU wobble base pairs are shifted downfield, whereas resonances from FU:A base pairs shift upfield.

Spectral changes produced by the binding of EB to the (FUra)minihelix show that the three upfield resonances, corresponding to base pairs FU4:A69, FU67:A6 and FU7:A66, are not affected by EB binding (Fig. 7). This indicates that EB does not intercalate between base pairs 7:66 and 6:67 of the minihelix as it does in intact tRNA^{Val}. As EB concentration is increased, resonances in the central region of the spectrum, corresponding to FUra residues in the loop region and peak A (FU64) shift. Splitting of peak A is also observed, indicating that FU64 is in slow exchange between two environments, free and EB bound. The signal from the dye-bound state resonates 0.11 p.p.m. upfield from that in the dye-free molecule.

DISCUSSION

The ^{19}F NMR chemical shifts of free and EB bound (FUra)tRNA^{Val} are summarized in Table 1. Chemical shift differences of FU67 and FU7 (located at the base of the acceptor stem) between free and EB-bound tRNA are 0.54 and 0.74 p.p.m., respectively, at 22°C. A secondary EB binding site is observed at the FU4:A69 base pair. The ^{19}F chemical shift difference between the EB-complexed and free form at this site is only 0.27 p.p.m., suggesting that dye binding is not as strong as it is between base pairs FU67:A6 and FU7:A66. Increasing the temperature to 47°C does not affect the affinity of EB to the acceptor stem of the tRNA (Table 1). No other major changes in chemical shift are observed in the intact tRNA molecule except for small shifts (0.09 p.p.m.) of FU47 at higher EB concentrations (Figs 2 and 3). It is difficult to determine whether this shift is in slow or fast exchange. It does

suggest that EB may have a weak non-intercalating binding site in this region of the tRNA molecule.

Our results agree with those of previous proton NMR (12,13) and fluorescence (14–16) studies, which suggested that EB binds to tRNA by intercalation into the acceptor stem. However, both our ^{19}F NMR studies and the ^{1}H NMR studies of tRNA^{Val} show evidence for more than one EB binding site located in the acceptor stem under our experimental conditions; earlier proton NMR studies (12,13) detected a unique EB binding site in the acceptor stem. X-ray diffraction study of crystals of an EB–tRNA complex indicated that EB stacks over U8 in the P-10 loop of the tRNA structure (17). Neither the proton NMR studies by Kearns and co-workers (12,13), nor the ^{19}F NMR studies reported here detect significant binding of EB in the tertiary structure of the tRNA molecule; in particular, there is no evidence for EB interaction with U8. The single crystal study may have failed to detect the intercalative binding of EB because dye was bound to the tRNA after crystal formation. Under these conditions (soaking pre-formed tRNA crystals in EB solution), the ligand may prefer to bind to fast exchange sites, perhaps the weaker tertiary binding site. ^{31}P NMR studies also support the binding of EB in the tertiary structure region (18). The ^{31}P NMR spectrum of tRNA^{Phe} was, however, not completely assigned, adding to the uncertainty of the EB binding sites in the tRNA molecule.

Both our ^{19}F and ^{1}H NMR studies agree that EB intercalates between base pairs from 4:69 to 7:66 in the acceptor stem of the tRNA^{Val} molecule. The selective binding of EB to tRNA prompted us to ask whether this binding is sequence specific or whether there is a structural requirement for EB binding. To help answer this question, a minihelix corresponding to the acceptor stem and the T-arm of tRNA^{Val} was synthesized. This truncated structure contains the EB binding site of the full length tRNA molecule. ^{19}F and ^{1}H NMR spectra of the fluorinated minihelix show that this sequence forms a 12 base-paired helical stem. There are two possible structures that cannot be distinguished by the NMR data, a monomeric hairpin helix or an intermolecular duplex dimer, as suggested by Aboul-ela and co-workers (39). Gel permeation chromatography of the minihelix indicates it exists as a monomer in solution, ruling out the latter possibility.

Both ^{19}F and ^{1}H NMR studies show that addition of EB to the minihelix no longer involves base pairs 4:69–7:66, the EB binding sites in the intact tRNA^{Val} molecule. ^{1}H NMR (Fig. 5) shows that the EB binding site has shifted to base pairs G50:FU64-G53:C61 of the minihelix, adjacent to the single-stranded loop region. Intercalation of EB at the base of the stem also affects the structure of the single-stranded region as seen by the spectral changes in the central region of the ^{19}F NMR spectrum (Fig. 7).

The results presented in this study suggest that binding of EB to the RNA molecule is not sequence specific. EB is likely to have a structural preference for binding to the base of a helical stem.

ACKNOWLEDGEMENTS

We thank Ms Shimin Li for technical support and Dr R. D. Scott for assistance with the NMR instrumentation. The 500 MHz NMR instrument is part of the Biotechnology Instrumentation Facilities at Iowa State University. Support for this investigation was provided by NIH grant GM-45546 and NSF grant MCB 95-13932. This is Journal Paper No. J-17372 of the Iowa Agriculture and Home Economics Experiment Station, Ames, IA, Project No. 3131, supported by Hatch Act and State of Iowa funds.

REFERENCES

1 Waring, M.J. (1975) In Corcoran, J.W. and Hahn, F.E. (eds), *Antibiotics III*. Springer-Verlag, New York, pp. 141–165.
2 Dickenson, L., Chantrill, D.I., Inkley, G.W. and Thompson, M.J. (1953) *Br. J. Pharmacol.* **8**, 139–142.
3 Eron, L.J. and McAuslan, B.R. (1966) *Biochim. Biophys. Acta* **114**, 633–636.
4 Lurquin, P. and Buchet-Mahieu, J. (1971) *FEBS Lett.* **12**, 244–248.
5 Kramer, F.R., Mills, D.R., Cole, P.E., Nishihara, T. and Spiegelman, S. (1974) *J. Mol. Biol.* **89**, 719–736.
6 Loeb, L.A. (1974) In Boyer, P.D. (ed), *Enzymes*, 3rd edn. Academic Press, NY, Vol. **10**, pp. 173–209.
7 Waring, M.J. (1964) *Biochim. Biophys. Acta* **87**, 358–361.
8 Waring, M.J. (1965) *J. Mol. Biol.* **13**, 269–282.
9 Bauer, W. and Vinograd, J. (1968) *J. Mol. Biol.* **33**, 141–171.
10 Kreishman, G.P., Chan, S.I. and Bauer, W. (1971) *J. Mol. Biol.* **61**, 45–58.
11 Neidle, S. and Abraham, Z. (1984) *CRC Crit. Rev. Biochem.* **17**, 73–121.
12 Jones, C.R. and Kearns, D.R. (1975) *Biochemistry* **14**, 2660–2665.
13 Jones, C.R., Bolton, P.H. and Kearns, D.R. (1978) *Biochemistry* **17**, 601–607.
14 Bittman, R. (1969) *J. Mol. Biol.* **46**, 251–268.
15 Tao, T., Nelson, J.H. and Cantor, C.R. (1970) *Biochemistry* **9**, 3514–3524.
16 Wells, B.D. and Cantor, C.R. (1977) *Nucleic Acids Res.* **4**, 1667–1680.
17 Liebman, M., Rubin, J. and Sundaralingam, M. (1977) *Proc. Natl. Acad. Sci. USA* **74**, 4821–4825.
18 Goldfield, E.M., Luxon, B.A., Bowie, V. and Gorenstein, D.G. (1983) *Biochemistry* **22**, 3336–3344.
19 Nielsen, P.E. (1981) *Biochim. Biophys. Acta* **655**, 89–95.
20 Horowitz, J., Ofengand, J., Daniel, W.E. and Cohn, M. (1977) *J. Biol. Chem.* **252**, 4418–4420.
21 Hardin, C.C., Gollnick, P., Kallenbach, N.R., Cohn, M. and Horowitz, J. (1986) *Biochemistry* **25**, 5699–5709.
22 Hardin, C.C., Gollnick, P. and Horowitz, J. (1988) *Biochemistry* **27**, 487–495.
23 Gollnick, P., Hardin. C.C. and Horowitz, J. (1986) *Nucleic Acids Res.* **14**, 4659–4672.
24 Gollnick, P., Hardin, C.C. and Horowitz, J. (1987) *J. Mol. Biol.* **197**, 571–589.
25 Chu, W.-C. and Horowitz, J. (1989) *Nucleic Acids Res.* **17**, 7241–7252.
26 Chu, W.-C. and Horowitz, J. (1991) *Biochemistry* **30**, 1655–1663.
27 Chu, W.-C. and Horowitz, J. (1991) *FEBS Lett.* **295**, 159–162.
28 Chu, W.-C., Feiz, V., Derrick, W.B. and Horowitz, J. (1992) *J. Mol. Biol.* **227**, 1164- 1172.
29 Chu, W.-C., Kintanar, A. and Horowitz, J. (1992) *J. Mol. Biol.* **227**, 1173–1181.
30 Liu, M. and Horowitz, J (1993) *BioTechniques* **15**, 264–266.
31 Nakamaye, K.L. and Eckstein, F. (1986) *Nucleic Acids Res.* **14**, 9679–9698.
32 Shaw, D. (1976) In *Fourier Transform NMR Spectroscopy*. Elsevier, New York, p 179.
33 Kintanar, A., Metzler, C.M., Metzler, D.E. and Scott, R.D. (1991) *J. Biol. Chem.* **266** 17222–17229.
34 Sklenar, V. and Bax, A. (1987) *J. Magn. Reson.* **74**, 469–479.
35 Plateau, P. and Guéron, M. (1982) *J. Am. Chem. Soc.* **104**, 7310–7311.
36 Kintanar, A., Yue, D. and Horowitz, J. (1994) *Biochimie* **76**, 1192–1204.
37 Sander, E.G. and Deyrup, C.L. (1972) *Arch. Biochem. Biophys.* **150**, 600–605.
38 Holbrook, S.R., Sussman, J.L., Warant, R.W. and Kim, S.-H. (1978) *J. Mol. Biol.* **123**, 631–660.
39 Aboul-ela, F., Nikonowicz, E.P. and Pardi, A. (1994) *FEBS Lett.* **347**, 261–254.